Comparison of the Maxwell and Boltzmann theory for multilayered dielectric random media

S. Menon, Q. Su, and R. Grobe
Intense Laser Physics Theory Unit and Department of Physics, Illinois State University, Normal, Illinois 61790-4560
(Received 4 September 2001; published 17 May 2002)

Based on the transfer matrix theory for electromagnetic fields, we develop a corresponding theory for intensity transport in a one-dimensional random medium. We show the conditions for which the Maxwell equations, the intensity transport theory, and the Boltzmann equation can lead to similar predictions. We generalize the transfer matrix theory to study intensity modulated waves and compare its predictions with those obtained from the Maxwell and Boltzmann equations.

DOI: 10.1103/PhysRevE.65.051917 PACS number(s): 87.90.+y, 05.60.−k, 42.62.Be

I. INTRODUCTION

The propagation of electromagnetic fields through highly scattering media is a subject of interest in many areas of science [1,2]. The Maxwell equations give a very accurate description of the interaction of fields with these media at a microscopic level and explicitly takes interference, diffraction, and polarization effects into account. The radiative energy transfer (Boltzmann) equation has been used to explain various phenomena in astrophysics [1], atmospheric sciences, oceanography, and biophysics [2]. It treats waves as a transport of particles or energy and neglects any correlation or interference effects. This equation, however, can be derived only from phenomenological considerations and its rigorous derivation even from the basic scalar wave Maxwell equation is not available [3].

The precise relationship between the Maxwell and Boltzmann equations is still an open question. The two descriptions are known to be related for the special cases of stationary and homogenous free fields in the absence of any turbid medium [4]. Nonetheless, many important questions remain to be answered. For example, given a random collection of scatterers, is there a parameter regime for which the Maxwell and the Boltzmann equations predict similar results? To our knowledge, even for a simple one-dimensional system of random scatterers, a relationship between both theories is not known. A comparative study of the Maxwell and Boltzmann equations has relevance in areas where the Boltzmann equation is extensively used to model experimental results. For example, important medical applications of the scattering properties of near infrared light have been explored recently for biological tissues [5]. These include spectroscopic [6,7] and other noninvasive [8–16] techniques to identify abnormal tissue behavior. High-frequency radiation like visible light loses its coherence within a few scattering lengths in a turbid medium. However, if the radiation source is modulated in time, the coherence associated with the modulated component is retained upto larger distances [12] and is useful for characterizing a turbid medium. A modulated source in a turbid medium can give rise to photon density waves that have some of the usual wavelike properties and have been discussed extensively for applications in medical diagnostics [12–16]. A nice overview of recent applications and insight of the photon density waves are given in Ref. [17].

These experiments are usually modeled using the Boltzmann transport equation [18]. Under suitable approximations, the Boltzmann equation reduces to the diffusion model [19] that has analytical solutions and thus is more appealing [11–16]. However, to test the validity of these approximations and the Boltzmann equation itself, a suitable technique has to be developed for comparison with the Maxwell equations.

The main aim of this work is to report some conditions under which the solutions of the Maxwell equations agree with the predictions of the Boltzmann equation. For simplicity, we will consider a multilayered dielectric medium that scatters preferentially in the forward or backward direction. The advantage such a medium offers is that the solutions of Maxwell equations can be obtained from simple transfer matrices without the unnecessary complications associated with higher dimensions.

The organization of this paper is as follows. In Sec. II we introduce our turbid medium and revisit the transfer matrix theory and discuss the exact transmission coefficients. In Sec. III we develop an approximate theory for the intensity transport based on the transfer matrices for the electric field. We show that the intensity transfer matrix theory is similar to the Boltzmann equation. We then discuss the parameter regime where the ensemble averaged solution of the Maxwell equations is related to the Boltzmann equation. In Sec. IV we derive a microscopic transfer matrix approach for intensity modulated waves and compare the Maxwell and the Boltzmann theory for these waves. We conclude with a short summary in Sec. V.

II. EXACT SOLUTION OF THE MAXWELL EQUATIONS USING TRANSFER MATRICES

The random medium whose optical propagation properties we will examine in this work consists of a series of N lossless plane-parallel dielectric layers arranged perpendicular to the z axis. The jth layer is centered at position z_j, has a width d_j and an index of refraction n_j $(j=1,N)$ as shown in Fig. 1. To simulate a turbid medium the numerical values for these parameters were chosen randomly with uniform distributions. In our calculations we take a ''glasslike'' index of refraction in the range $1.3<n_j<1.5$. The distance between the center of the jth and $(j+1)$th layer is denoted by Δz_j and we take the range $0.5<\Delta z_j/\langle\Delta z\rangle<1.5$. For numerical purposes we will measure all lengths in units of $\langle\Delta z\rangle$, which

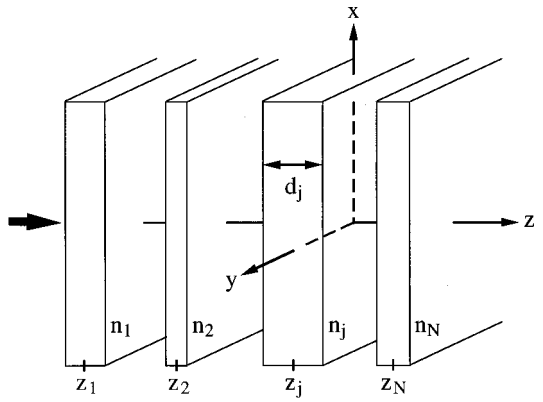

FIG. 1. Sketch of the multilayered dielectric turbid medium. The laser light is polarized along the *y* direction and is injected perpendicular to the interface of the first slab.

is the average separation between the centers of two neighboring layers. We neglect any homogeneous dispersion arising from a wavelength dependent index of refraction. However, we will show that due to the arrangement of the slabs the total transmission depends very strongly on the wavelength.

We assume that the incoming electromagnetic field travels along the *z* axis perpendicular to the interfaces. This allows us to analyze the dynamics strictly in one dimension where the scattering is restricted to either reflection or transmission, and we consider the electric field vector parallel to the glass-vacuum interfaces. Due to this geometry, the problem can be investigated numerically using the transfer matrix approach by matching electric fields at the interfaces [20,21]. In general, the electric field is a superposition of plane waves and we denote each plane wave as $\mathbf{E}=\mathbf{e}_y E e^{i(\pm kz-\omega t)}$, where E is the complex amplitude polarized along the $\mathbf{e}_y$ direction and $k=2\pi/\lambda$ denotes the wave number of the field. The field propagates in the positive or negative *z* direction depending on the sign in the exponent.

For the jth slab, the amplitudes of the fields traveling towards the slab along the positive and negative *z* direction are denoted by E_a and E_d and the fields leaving the slab by E_c and E_b, respectively. Using the continuity conditions for the electric and magnetic field components at each of the two interfaces at $z_j \pm d_j/2$, the outgoing and incoming fields can be related by

$$E_c = t_j E_a - \frac{r_j^* t_j}{t_j^*} E_d, \tag{2.1a}$$

$$E_b = r_j E_a + t_j E_d, \tag{2.1b}$$

where $r_j=\sqrt{R_j}\exp[i(2kz_j+\phi_j+\pi/2)]$ and $t_j=\sqrt{T_j}e^{i\phi_j}$ are the complex reflection and transmission amplitudes.

$$T_j = \frac{4n_j^2}{4n_j^2\cos^2 kn_j d_j + (n_j^2+1)^2 \sin^2 kn_j d_j} \tag{2.2}$$

is the real transmission coefficient and the phase is

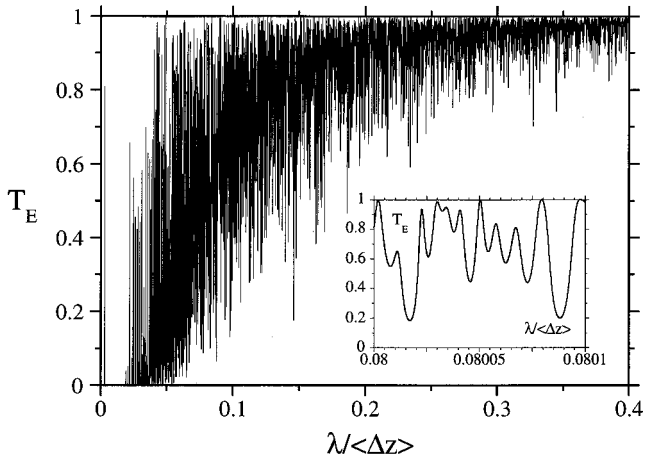

FIG. 2. The transmission coefficient T_E as a function of wavelength for a medium of $N=500$ scatterers. The disorder present in n_j, d_j, and z_j varied in the range $1.3<n_j<1.5$, $0.5<\Delta z_j/\langle\Delta z\rangle<1.5$, and $0.0009<d_j/\langle\Delta z\rangle<0.0011$. The graph is displayed with only 2000 points, while the transmission, due to resonances, is a very rapidly oscillating function of the wavelength. The true scale of these oscillations is shown in the inset.

$$\phi_j = \tan^{-1}\{(n_j^2+1)\tan(n_j k d_j)/2n_j\} - k d_j. \tag{2.3}$$

As the medium is lossless the transmission and reflection coefficients are related via $T_j+R_j=1$. The field amplitudes on the left and right side of the jth slab can be related through

$$\begin{pmatrix} E_c \\ E_d \end{pmatrix} = \mathbf{M}_{\mathbf{E}j} \begin{pmatrix} E_a \\ E_b \end{pmatrix}, \tag{2.4}$$

where $\mathbf{M}_{\mathbf{E}j}$ is the transfer matrix for the jth slab given by

$$\mathbf{M}_{\mathbf{E}j} = \begin{pmatrix} 1/t_j^* & -r_j^*/t_j^* \\ -r_j/t_j & 1/t_j \end{pmatrix}. \tag{2.5}$$

Thus the matrix $\mathbf{M}_{\mathbf{E}j}$ characterizes the field transported by each slab ($j=1,2,\ldots,N$). In between the slabs, the electric field amplitude does not change and the outgoing wave E_c of the slab at z_j is identical to the incoming field E_a of the slab at z_{j+1}. Thus for a medium comprised of N slabs, the transfer matrix of the medium can be obtained by multiplying the noncommuting matrices numerically, $\mathbf{M}_{\mathbf{E}} = \mathbf{M}_{\mathbf{E}N}\mathbf{M}_{\mathbf{E}N-1}\cdots\mathbf{M}_{\mathbf{E}1}$. The total reflection and transmission coefficients for the entire medium can be computed from the product matrix $\mathbf{M}_{\mathbf{E}}$ via $R_E=|-\mathbf{M}_{\mathbf{E}}(2,1)/\mathbf{M}_{\mathbf{E}}(2,2)|^2$ and $T_E = |\det(\mathbf{M}_{\mathbf{E}})/\mathbf{M}_{\mathbf{E}}(2,2)|^2$, where $\mathbf{M}_{\mathbf{E}}(n,m)$ denote the four matrix elements of $\mathbf{M}_{\mathbf{E}}$.

In Fig. 2 we show the transmission T_E as a function of the wavelength for a typical random medium of $N=500$ scatterers. For very small wavelengths ($\lambda<0.02$) the transmission is very small due to destructive interference. This is the photonic band gap or the localization regime for a 1D medium [22]. Beyond the band-gap regime the transmission is characterized by many interferences and it is very sensitive to the wavelength, as apparent by the oscillatory graph. Even

though there is an overall tendency of the medium to become more transparent with increasing laser wavelength, the large size of the fluctuations indicates the importance of the interferences between the individual scatterers for strictly monochromatic fields. The inset resolves these rapid oscillations on a very fine wavelength scale. It is quite remarkable that an increase of the wavelength from $\lambda = 8.008 \times 10^{-2}$ (with $T_E = 1$) by only $\Delta\lambda/\lambda = 0.01\%$ to $\lambda = 8.009 \times 10^{-2}$ ($T_E = 0.2$) changes the optical transmission from perfectly transparent to nearly opaque. As the transmission coefficient is so sensitively determined by interferences, one might (incorrectly) conjecture that the Boltzmann theory that does not incorporate any wavelike phenomena should be completely inapplicable for this one-dimensional medium comprised of 500 glass layers. In the following section we will demonstrate that this conjecture is surprisingly incorrect.

III. THEORIES FOR THE ELECTROMAGNETIC WAVES

A. Intensity transfer matrix theory

Before we proceed to the comparison with the Boltzmann equation, we develop a transfer matrix theory for the intensity transport. As we will show, such a theory compares well with the Boltzmann equation and provides the link between the optical characteristics of the individual scatterers and macroscopic quantities required for the Boltzmann equation. The intensity corresponding to a complex plane wave is defined as $I \equiv (c\varepsilon/2)\mathbf{E}\cdot\mathbf{E}^*$ where c is the speed of the field and ε is the electric permittivity of the medium, respectively. Using Eq. (2.1), the corresponding equations for the intensity can be written as

$$I_c = T_j I_a + R_j I_d - \frac{c\varepsilon}{2}(r_j^* t_j E_d E_a^* + \text{c.c.})$$

$$= T_j I_a + R_j I_d + c\varepsilon\sqrt{R_j T_j}\sin(2kz_j + \theta)|E_d||E_a|, \quad (3.1a)$$

$$I_b = R_j I_a + T_j I_d + \frac{c\varepsilon}{2}(r_j^* t_j E_d E_a^* + \text{c.c.})$$

$$= R_j I_a + T_j I_a - c\varepsilon\sqrt{R_j T_j}\sin(2kz_j + \theta)|E_d||E_a|, \quad (3.1b)$$

where θ is the relative phase between the input fields E_d and E_a. The cross terms oscillate at $2k$ and are associated with the interference between E_a and E_d. The key, and only, approximation we will use to derive the intensity theory is that we will neglect the interference terms in Eq. (3.1). The corresponding transfer matrix connecting the intensities on the left (I_a, I_b) with the intensities on the right (I_c, I_d) takes the form

$$\mathbf{M_{I}}_j = \begin{pmatrix} T_j - R_j^2/T_j & R_j/T_j \\ -R_j/T_j & 1/T_j \end{pmatrix}. \quad (3.2)$$

It should be noted that this matrix does not contain the phase ϕ_j, as it depends only on the absolute value of the transmission and reflection amplitudes. The real transmission (T_I) or reflection (R_I) coefficient for the medium can be computed from the product of the matrices $\mathbf{M_I} = \mathbf{M_{I}}_N \mathbf{M_{I}}_{N-1} \cdots \mathbf{M_{I}}_1$ in the same way as T_E and R_E were derived above from the matrix elements of $\mathbf{M_E}$.

B. The Boltzmann theory for multilayered media

In the absence of absorption the general form of the one-speed Boltzmann equation (radiative transfer equation) is given by [1,2]

$$\left[\frac{\partial}{c\partial t} + \mathbf{\Omega}\cdot\boldsymbol{\nabla}\right] I(\mathbf{r},t,\mathbf{\Omega}) = \mu_s \int d\mathbf{\Omega}' p(\mathbf{\Omega},\mathbf{\Omega}') I(\mathbf{r},t,\mathbf{\Omega}') - \mu_s I(\mathbf{r},t,\mathbf{\Omega}), \quad (3.3)$$

where μ_s is the scattering coefficient, $I(\mathbf{r},t,\mathbf{\Omega})$ is the intensity, $p(\mathbf{\Omega},\mathbf{\Omega}')$ is the conditional probability that the intensity propagating along $\mathbf{\Omega}$ direction is scattered in the $\mathbf{\Omega}'$ direction, and β is the scattering angle given by $\mathbf{\Omega}\cdot\mathbf{\Omega}' = \cos\beta$. We denote the average cosine of this angle by g, also known as the anisotropy factor. To model our multilayered medium we consider the scattering phase function [23]

$$p(\mathbf{\Omega},\mathbf{\Omega}') = \frac{1}{2\pi}\left[\frac{(1-g)}{2}\delta(\cos\beta + 1) + \frac{(1+g)}{2}\delta(\cos\beta - 1)\right]. \quad (3.4)$$

This phase function reflects the geometry of our slabs and allows scattering only in the forward or backward direction. The Boltzmann equation simplifies to

$$\left(\frac{\partial}{c\partial t} + \frac{\partial}{\partial z}\right) I(z,t,+) = -\mu\{I(z,t,+) - I(z,t,-)\}, \quad (3.5a)$$

$$\left(\frac{\partial}{c\partial t} - \frac{\partial}{\partial z}\right) I(z,t,-) = \mu\{I(z,t,+) - I(z,t,-)\}, \quad (3.5b)$$

where $I(z,t,+)$ and $I(z,t,-)$ are the intensities along the positive and negative z direction and the reduced scattering coefficient is defined as $\mu \equiv (1-g)/2\ \mu_s$. Under a steady state condition the total reflection and transmission coefficients for a medium of length W are defined as $T_B = |I(W,\infty,+)/I(0,\infty,+)|$ and $R_B = |I(0,\infty,-)/I(0,\infty,+)|$. We solve Eq. (3.5) with the boundary conditions $I(0,,+) = 1$ and $I(W,\infty,-) = 0$ and obtain the following solution for the Boltzmann equation transmission coefficient T_B [23]:

$$T_B = 1/(1+\mu W). \quad (3.6)$$

As the next step we have to relate the macroscopic Boltzmann parameters μ_s and g to the set of $3N$ microscopic parameters z_j, n_j, and d_j $(j = 1,2,\ldots,N)$ and to the density of the scatterers N/W. As the Boltzmann equation describes the medium only on a macroscopic level, we have to define the average transmission coefficient per slab, $T_{\text{ave}} \equiv (1/N)\Sigma_{j=1}^{N} T_j$. The anisotropy factor g should be directly related to the average scattering coefficient via

$$g = 2T_{\text{ave}} - 1. \tag{3.7a}$$

As a mathematically rigid microscopic derivation of the Boltzmann equation from the Maxwell equations is not available, the precise relation between μ_s and the parameter T_{ave} and the density of scatterers N/W is unknown in general. For our one-dimensional system we propose to identify μ_s with

$$\mu_s = N/(WT_{\text{ave}}). \tag{3.7b}$$

Relations (3.7) are the key link between the Boltzmann and Maxwell theory and the validity of these claims will be justified by the numerical examples to be discussed below. Using these two relations, the total transmission according to the Boltzmann equation T_B from Eq. (3.6) can be rewritten as

$$T_B = T_{\text{ave}}/[T_{\text{ave}} + N(1 - T_{\text{ave}})]. \tag{3.8}$$

We might note that this expression is identical to the one that would be obtained from the microscopic intensity theory presented in the preceding section for an ''average'' medium in which the N random scatterers are replaced with N effective scatterers having identical transmission coefficients $T_j = T_{\text{ave}}$. For this special case the product matrix $\mathbf{M_I} = \mathbf{M_{I}}_N \mathbf{M_{I}}_{N-1} \cdots \mathbf{M_{I}}_1$ can be evaluated analytically and we would find that the total transmission for this medium is given by $T_I = T_{\text{ave}}/[T_{\text{ave}} + N(1 - T_{\text{ave}})]$ in agreement with the result (3.8) obtained directly from the Boltzmann equation. This is a strong indication that the proposed relations (3.7) are reasonable. In other words, for a medium with low degree of disorder we expect the intensity and the Boltzmann theory to agree perfectly for monochromatic fields [24].

Let us now compare the three different approaches and evaluate the total transmission coefficients numerically. In Fig. 3(a) we plot the transmission from the Maxwell equations (2.5) (solid curve), the intensity theory (3.2) (dot-dashed curve), and the solution of Boltzmann equation (3.8) (dotted curve) for an identical microscopic medium with $N = 500$ random scatterers. As we saw in Fig. 2 for the same random medium, the transmission T_E predicted by Eq. (2.5) has strong interference contributions for a single medium. The curve displayed in Fig. 3 labeled $\langle T_E \rangle$ was obtained by averaging T_E over 10 000 media with $N = 500$ random scatterers each. This ensemble average removes the sharp resonances seen in Fig. 2. Numerically, the graph $\langle T_E \rangle$ was obtained by multiplying 500 (2×2) matrices 10^4 times for each of the 2000 values of the wavelength that takes a considerable amount of CPU time.

Good agreement is found between all three theories for $\lambda > 0.1$. In this regime the maximum difference between $\langle T_E \rangle$, T_I, and T_B is less than 1%. For smaller wavelength $(\lambda < 0.1)$ the agreement between the exact transmission $\langle T_E \rangle$ and the two approximations T_I and T_B gets slightly worse, but the overall qualitative agreement extending over the entire range of the transmission coefficient is remarkable. This validates the neglect of the interference terms in the derivation of the intensity theory and also the matching relations for the Boltzmann theory.

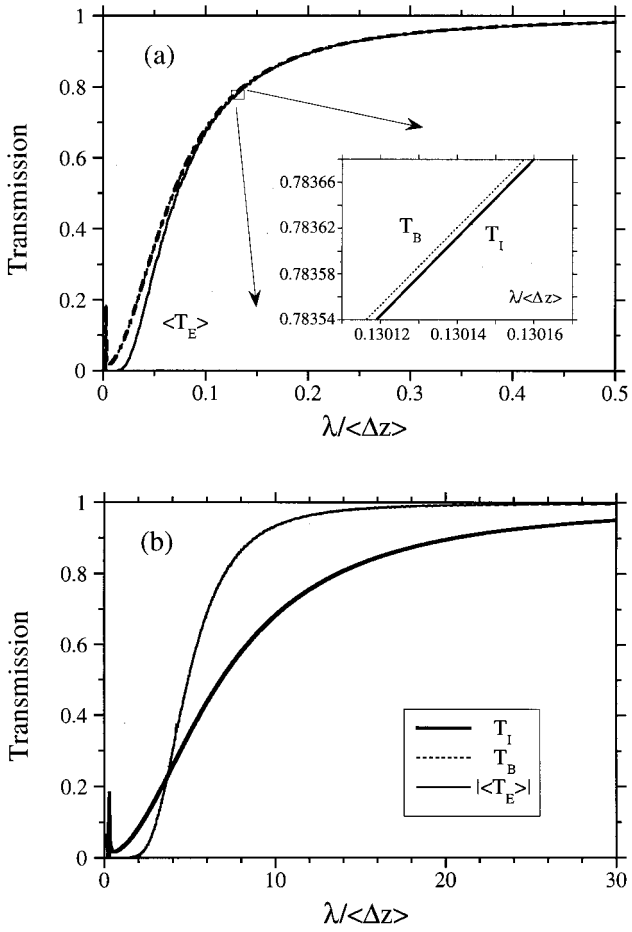

FIG. 3. Comparison between the prediction of the averaged $\langle T_E \rangle$ over 10 000 media (solid curve), solution of the Boltzmann equation T_B (dashed curve), and the intensity transfer matrix theory T_I (gray curve) as a function of wavelength for $N = 500$ random scatterers. In (a) the scatterers take random values in the range $1.3 < n_j < 1.5$, $0.5 < \Delta z_j/\langle \Delta z \rangle < 1.5$, and $0.0009 < d_j/\langle \Delta z \rangle < 0.0011$, corresponding to $\gamma = 1000$. In (b) all the parameters are the same but d_j varies in the range $0.09 < d_j/\langle \Delta z \rangle < 0.11$ corresponding to $\gamma = 10$.

Intuitively, one would expect that increasing the number of scatterers for wavelengths outside the localization regime, should average the interference effects to zero. On the contrary, various simulations for different parameter regimes suggest that increasing the number of scatterers does not necessarily lead to a better agreement between $\langle T_E \rangle$ and T_I. We find that the ratio of average spacing between the slabs to the average slab thickness, $\gamma \equiv \langle \Delta z \rangle / \langle d \rangle$, is a better measure for the validity of the intensity theory. The numerical data presented in Fig. 3(a) were for $\gamma = 1000$ and suggest that the Boltzmann theory is a good approximation to the ensemble averaged solutions of the Maxwell equations.

A regime where interference effects cannot be ''removed'' by ensemble averaging is shown in Fig. 3(b) where $\gamma = 10$ was too small. The predictions of $\langle T_E \rangle$, in Fig. 3(b), are either larger or smaller than T_I depending on whether there is, on average, a strong constructive or destructive interference in the transmission. Thus the Boltzmann theory is a

poor approximation for a medium with $\gamma \ll 100$. We have repeated these numerical calculations for ensembles associated with a wide range of γ between 10^3 and 10^6, and the resulting transmission curve remains nearly shape invariant, only the corresponding wavelength scale for the graph needs to be decreased with increasing γ.

In both figures, however, the transmission T_I predicted by the intensity transfer matrix theory and the macroscopic description of the Boltzmann equation T_B is extremely good. We have numerically verified that even for individual T_j varying from 0.6 to 0.99, T_I and T_B are in good agreement as is apparent in the blow up displayed in the inset. In Fig. 3(b), at $\lambda = 1$, the transmission coefficients of the individual scatterers varied from 0.887 to 0.967 and the average $T_{\text{ave}} \approx 0.934$. The relative error between T_I and T_B at $\lambda = 1$ in Fig. 3(b) is less than 0.7% and decreases rapidly with increasing wavelength because the variation of T_j about its average value also decreases. Also seen from both graphs in Figs. 3 is that the qualitative agreement between T_I and T_B seems to be rather independent of γ. Note that since interference effects have been dropped in the derivation of intensity theory, there is no band gap region for both T_I and T_B.

IV. THEORIES FOR INTENSITY MODULATED WAVES

In the following, we will derive a microscopic transfer matrix theory for intensity modulated waves and compare it with the solution of the ensemble averaged Maxwell equations and also with the Boltzmann transport theory. The intensity is modulated with a frequency $\omega_m = ck_m$, which is assumed to be much smaller than the carrier frequency $2\pi c/\lambda$. The corresponding electric field for such an intensity modulation can be given as a superposition of two monochromatic fields with wave numbers $k^{(1)} \equiv k + k_m/2$ and $k^{(2)} \equiv k - k_m/2$ with $k_m \ll k$.

$$\mathbf{E} = E^{(1)} e^{i(\pm k^{(1)} z - \omega^{(1)} t)} + E^{(2)} e^{i(\pm k^{(2)} z - \omega^{(2)} t)} \tag{4.1}$$

and the corresponding intensity is

$$I = \frac{c\varepsilon}{2}\{|E^{(1)}|^2 + |E^{(2)}|^2 + (E^{(1)} E^{(2)*} e^{i(\pm k_m z - \omega_m t)} + \text{c.c.})\}, \tag{4.2}$$

where the cross term is the modulated component of the intensity. We derive a theory that permits us to compute the reflection and transmission coefficient for this component. This can be performed at three different levels of approximation. Using the results of Sec. II we can compute the reflection and transmission coefficient exactly, which is essentially the electric field approach for each of the two monochromatic fields. On the other hand, following Sec. III A, an approximate intensity transfer matrix for each individual scatterer can be derived by neglecting the interference terms. The third approach will be to solve the Boltzmann equation analytically for intensity modulated waves using the correspondence relations (3.7).

A. Exact theory

It is clear from the discussion in Sec. II that a collection of N random scatterers is described by the transfer matrix $\mathbf{M_E}$. The corresponding total reflection and transmission amplitudes are denoted by $r^{(q)}$ and $t^{(q)}$ where $q = 1,2$ labels the two fields with wave numbers $k^{(1)}$ and $k^{(2)}$, respectively. Using Eq. (2.1) the two fields satisfy

$$E_c^{(q)} = t^{(q)} E_a^{(q)}, \quad E_b^{(q)} = r^{(q)} E_a^{(q)}, \tag{4.3}$$

where we use the fact that the input field $E_d^{(q)}$ at the right end of the medium is zero. The equations for intensities I_c and I_b coming in and out of the medium are

$$I_c = I_c^{(1)} + I_c^{(2)} + (J_c e^{i(k_m z - \omega_m t)} + \text{c.c.}), \tag{4.4a}$$

$$I_b = I_b^{(1)} + I_b^{(2)} + (J_b e^{i(-k_m z - \omega_m t)} + \text{c.c.}), \tag{4.4b}$$

where $J_p \equiv (c\varepsilon/2) E_p^{(1)} E_p^{(2)*}$ $[p = a,b,c,d]$ denotes the modulated component of the intensity. Using Eq. (4.3) and equating terms with the same time dependence, the effective reflection and transmission coefficients for the modulated component are $R_E = r^{(1)} r^{(2)*}$ and $T_E = t^{(1)} t^{(2)*}$. Both $r^{(q)}$ and $t^{(q)}$ can be calculated numerically from the matrix product (2.5), resulting in the exact transmission and reflection coefficient for the intensity modulated component. All the interference effects and the exact phase of the reflected and transmitted intensity are included in this approach. The modulated intensity is complex and the sum $|R_E| + |T_E|$ does not necessarily equate to unity, since it does not correspond to the total energy.

B. Approximate transfer matrix for individual scatterers

We now derive an approximate microscopic transfer matrix involving individual scatterers for the modulated component of intensity. It follows from Eq. (2.1) that the $k^{(1)}$ and $k^{(2)}$ components of the fields for the jth scatterer at $z = z_j$ satisfy the following relations:

$$E_c^{(q)} = t_j^{(q)} E_a^{(q)} - \frac{r_j^{(q)*} t_j^{(q)}}{t_j^{(q)*}} E_d^{(q)}, \tag{4.5a}$$

$$E_b^{(q)} = r_j^{(q)} E_a^{(q)} + t_j^{(q)} E_d^{(q)}, \tag{4.5b}$$

where $t_j^{(q)}$ and $r_j^{(q)}$ are the transmission and reflection amplitudes of the jth slab. Substituting Eq. (4.5) in Eq. (4.4) and equating the time dependent terms the following equalities can be derived:

$$J_c = T_{Mj} J_a + \frac{R_{Mj}^* T_{Mj}}{T_{Mj}^*} J_d - \frac{c\varepsilon}{2} \frac{T_{Mj} r_j^{(1)*}}{t_j^{(1)*}} E_d^{(1)} E_a^{(2)*} - \frac{c\varepsilon}{2} \frac{T_{Mj} r_j^{(2)}}{t_j^{(2)}} E_a^{(1)} E_d^{(2)*}, \tag{4.6a}$$

$$J_b = R_{Mj} J_a + T_{Mj} J_d + \frac{c\varepsilon}{2} t_j^{(1)} r_j^{(2)*} E_d^{(1)} E_a^{(2)*} + \frac{c\varepsilon}{2} r_j^{(1)} t_j^{(2)*} E_a^{(1)} E_d^{(2)*}, \quad (4.6b)$$

where $R_{Mj} \equiv \sqrt{R_j^{(1)} R_j^{(2)}} e^{i(k_m z_j + \varphi_j)}$, $T_{Mj} \equiv \sqrt{T_j^{(1)} T_j^{(2)}} e^{i\varphi_j}$, and $\varphi_j \equiv \phi_j^{(1)} - \phi_j^{(2)}$. For the special case of $\omega_m = 0$ the complex transmission coefficient reduces to $T_{Mj} = T_j$, which was defined in Eq. (2.2). The cross terms can be rewritten as

$$J_c = T_{Mj} J_a + \frac{R_{Mj}^* T_{Mj}}{T_{Mj}^*} J_d + \frac{ic\varepsilon}{2} \sqrt{R_j^{(1)} T_j^{(2)}} E_d^{(1)} E_a^{(2)*} e^{-i(2k^{(1)} z_j - \varphi_j)} - \frac{ic\varepsilon}{2} \sqrt{R_j^{(2)} T_j^{(1)}} E_a^{(1)} E_d^{(2)*} e^{i(2k^{(2)} z_j + \varphi_j)}, \quad (4.7a)$$

$$J_b = R_{Mj} J_a + T_{Mj} J_d - \frac{ic\varepsilon}{2} \sqrt{R_j^{(2)} T_j^{(1)}} E_d^{(1)} E_a^{(2)*} e^{-i(2k^{(2)} z_j - \varphi_j)} + \frac{ic\varepsilon}{2} \sqrt{R_j^{(1)} T_j^{(2)}} E_a^{(1)} E_d^{(2)*} e^{i(2k^{(1)} z_j + \varphi_j)}. \quad (4.7b)$$

The interference terms oscillate with high wave number $2k^{(1)}$ or $2k^{(2)}$. Under situations when such interference terms average to zero, the following transfer matrix for the modulated component can be constructed

$$\mathbf{M_{Ij}} = \begin{pmatrix} T_{Mj} - |R_{Mj}|^2 / T_{Mj}^* & R_{Mj}^* / T_{Mj}^* \\ -R_{Mj} / T_{Mj} & 1/T_{Mj} \end{pmatrix}, \quad (4.8)$$

where T_{Mj} and R_{Mj} are the complex transmission and reflection coefficients for each slab. The total transmission (T_I) and reflection (R_I) coefficient for N random scatterers can be determined from the matrix multiplication $\mathbf{M_I} = \mathbf{M_{IN}} \mathbf{M_{IN-1}} \cdots \mathbf{M_{I1}}$. note that the matrix (4.8) goes to matrix (3.2) when the modulation frequency $\omega_m = 0$ and the matrix elements are real numbers.

C. Predictions of the Boltzmann equation

The Boltzmann equation with an intensity modulated source is represented by the boundary conditions $I(z=0,t,+) = e^{i\omega_m t}$ and $I(W,t,-) = 0$. In Ref. [24] an analytical form for the reflection and transmission coefficients was derived,

$$T_B = \left| \frac{C^2 - ik_m(ik_m - 2\mu)S^2}{C - (ik_m - \mu)S} \right|, \quad (4.9a)$$

$$R_B = \left| \frac{S\mu}{C - (ik_m - \mu)S} \right|, \quad (4.9b)$$

where $C \equiv \cosh(\kappa W)$ and $S \equiv \sinh(\kappa W)/\kappa$ with $\kappa \equiv [-2i\mu k_m - k_m^2]^{1/2}$ and W is again the length of the medium. For the special case of a nonmodulated intensity, $k_m = 0$, Eqs. (4.9) reduce to the form given in Eq. (3.6). Continuing with the same procedure as outlined in Eq. (3.7), we relate μ to the average transmission coefficient and the total number of scatterers N. This time we define the average transmission $T_{\text{ave}} = (1/2N) \Sigma_{j=1}^{N} (T_j^{(1)} + T_j^{(2)})$ to represent $k^{(1)}$ and $k^{(2)}$ in the Boltzmann theory.

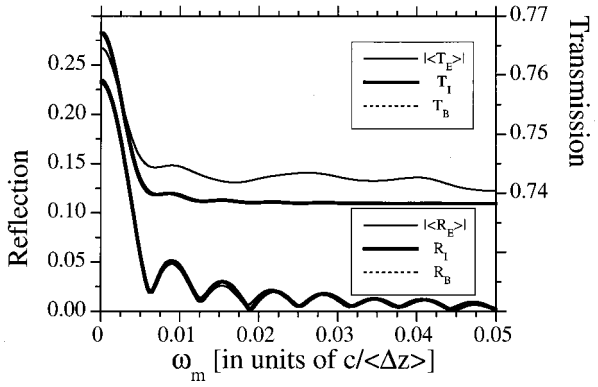

FIG. 4. The absolute values of the reflection (left y axis) and transmission (right y axis) coefficients for modulated intensities as a function of the modulation frequency ω_m in units of $c/\langle \Delta z \rangle$. The solid curves are for $|\langle R_E \rangle|$ and $|\langle T_E \rangle|$ averaged over 10 000 media. The gray curve for R_I and T_I, and the dashed curve for R_B and T_B are in full agreement. For all the curves, 500 scatterers were assigned the random values in the range $1.3 < n_j < 1.5$, $0.5 < \Delta z_j / \langle \Delta z \rangle < 1.5$, $0.0009 < d_j / \langle \Delta z \rangle < 0.0011$, and the carrier wavelength is $\lambda / \langle \Delta z \rangle = 2\pi/50$.

We have derived three different methods to calculate the reflection and transmission coefficients for an intensity modulated wave. Since the ensemble averaged quantities $\langle R_E \rangle$ and $\langle T_E \rangle$ are exact solutions of the Maxwell equations, they can be used to test the validity of matrix (4.8) and the results of the Boltzmann equation (4.9). In Fig. 4 the reflection and transmission coefficients obtained from the three methods are displayed as a function of the modulation frequency ω_m. We have selected a parameter regime ($\gamma = 1000$, $\lambda = 0.063$) where the Maxwell and Boltzmann theories are in agreement for a nonmodulated field ($\omega_m = 0$). As can be seen from the graphs, the agreement between the Boltzmann and intensity transfer matrix theory remains good even for modulated intensities. The solution of the Maxwell equations differs only quantatively and even the oscillations in $|\langle R_E \rangle|$ that can be associated with the finite width W of the medium are reproduced by R_I as well as R_B.

V. SUMMARY

We discussed the parameter regime for which the ensemble averaged solution of the Maxwell equations can be linked directly to the Boltzmann transport equation for monochromatic waves. We have also derived and tested a transfer matrix approach for the propagation of electromagnetic waves whose intensity is modulated. We again found a good agreement with the ensemble averaged Maxwell equations and Boltzmann equation if the average spacing between the scatterers is much larger than their width. This agreement is remarkable as one expects that for a one-dimensional (1D) medium the wave interferences would be most dominant compared to higher dimensional systems and therefore the

present system should not agree so well with the predictions of the Boltzmann theory as in 2D or 3D geometries.

For computational simplicity we have used a geometry that permitted us the use of the propagator solutions to the steady state Maxwell equations (transfer matrices). However, despite this restriction we point out that this medium can be realized experimentally using a sequence of plane parallel glass sheets with varying thickness and index of refraction as sketched in Fig. 1.

Even though we have shown that the intensity matrices are very helpful in linking the steady state solutions of the Boltzmann equation with the ensemble averaged solution of the Maxwell equations, we have not managed to show a possible relationship at the level of differential equations. Many more studies will be required to relate the microscopic and macroscopic approaches at the level of the equations of motion. As a first step in this direction it might be quite useful to derive from the Maxwell equations an appropriate set of differential equations, which describes the temporal and spatial evolution of the ensemble averaged laser intensity.

ACKNOWLEDGMENTS

This project is supported by the NSF. We also acknowledge support from the Research Corporation for Cottrell Science Awards and ISU for URGs.

[1] S. Chandrasekhar, *Radiative Transfer* (Clarendon, Oxford, 1950).
[2] A. Ishimaru, *Wave Propagation and Scattering in Random Media* (Academic, New York, 1978), Vols. 1 and 2.
[3] L. Mandel and E. Wolf, *Optical Coherence and Quantum Optics* (Cambridge University Press, Cambridge, 1995), Chap. 5.
[4] E. Wolf, Phys. Rev. D **13**, 869 (1979).
[5] A. Yodh and B. Chance, Phys. Today **48**(3), 34 (1995).
[6] B. Chance, S. Nioka, J. Kent, K. McCully, M. Fountain, R. Greenfield, and G. Holtom, Anal. Biochem. **174**, 698 (1988); D. T. Delpy, M. Cope, P. Van der Zee, S. Arridge, S. Wray, and J. Wyatt, Phys. Med. Biol. **33**, 1433 (1988).
[7] For a review see, B. B. Das, F. Liu, and R. R. Alfano, Rep. Prog. Phys. **60**, 227 (1997).
[8] J. R. Singer, F. A. Grunbaum, P. Kohn, and J. Zubelli, Science **248**, 990 (1990).
[9] D. A. Benaron *et al.*, J. Cereb. Blood Flow Metab. **20**, 469 (2000).
[10] A. K. Dunn, H. Bolay, M. A. Moskowitz, and D. A. Boas, J. Cereb. Blood Flow Metab. **21**, 195 (2001).
[11] P. N. den Outer, Th. M. Nieuwenhuizen, and Ad. Lagendijk, J. Opt. Soc. Am. A **10**, 1209 (1993).
[12] E. Gratton, W. Mantulin, M. J. van de Ven, J. Fishkin, M. Maris, and B. Chance, in *Peace Through Mind/Brain Science* (Hamamatsu Photonics, Bridgewater, NJ, 1990), p. 183; J. B. Fishkin, Ph.D. thesis, University of Illinois, 1994.
[13] D. A. Boas, M. A. O'Leary, B. Chance, and A. G. Yodh, Appl. Opt. **36**, 75 (1997).
[14] J. M. Schmitt, A. Knuttel, and J. R. Knudsen, J. Opt. Soc. Am. A **9**, 1832 (1992); A. Knuttel, J. M. Schmitt, and J. R. Knutson, Appl. Opt. **32**, 381 (1993).
[15] B. J. Tromberg, L. O. Svaasand, T. T. Tsay, and R. C. Haskell, Appl. Opt. **32**, 607 (1993).
[16] M. A. O'Leary, D. A. Boas, B. Chance, and A. G. Yodh, Phys. Rev. Lett. **69**, 2658 (1992); D. A. Boas, M. A. O'Leary, B. Chance, and A. G. Yodh, Phys. Rev. E **47**, R2999 (1993).
[17] A. Madelis, Phys. Today **53**(8), 29 (1995).
[18] K. Michielsen, H. De Raedt, J. Przeslawski, and N. Garcia, Phys. Rep. **304**, 89 (1998).
[19] For a recent review on multiple scattering theories see, M. C. van Rossum and T. M. Nieuwenhuizen, Rev. Mod. Phys. **71**, 313 (1999).
[20] See, for example, Chap. 9 in D. J. Griffiths, *Introduction to Electrodynamics* (Prentice Hall, Englewood Cliffs, NJ, 1999).
[21] For a numerical treatment of turbid media in higher dimensions, see W. Harshawardhan, Q. Su, and R. Grobe, Phys. Rev. E **62**, 8705 (2000).
[22] S. John, Phys. Rev. Lett. **53**, 2169 (1984); S. John, Phys. Today **44**(5), 32 (1991).
[23] Q. Su, G. H. Rutherford, W. Harshawardhan and R. Grobe, Laser Phys. **11**, 98 (2001).
[24] For an exception to this rule for bichromatic fields, see, P. J. Peverly, R. E. Wagner, G. H. Rutherford, M. Marsalli, Q. Su, and R. Grobe, Phys. Rev. E. **65**, 031908 (2002).